Published in final edited form as:
Environ Int. 2019 May ; 126: 377–386. doi:10.1016/j.envint.2019.02.024.

High-throughput screening and chemotype-enrichment analysis of ToxCast phase II chemicals evaluated for human sodium-iodide symporter (NIS) inhibition

Jun Wang[a,b], **Daniel R. Hallinger**[a], **Ashley S. Murr**[a], **Angela R. Buckalew**[a], **Ryan R. Lougee**[b,c], **Ann M. Richard**[c], **Susan C. Laws**[a,*], **Tammy E. Stoker**[a,*]

[a]Endocrine Toxicology Branch, Toxicity Assessment Division, National Health and Environmental Effects Research Laboratory, Office of Research and Development, U.S. Environmental Protection Agency, Research Triangle Park, NC, 27711, USA

[b]Oak Ridge Institute for Science and Education, U.S. Department of Energy, Oak Ridge, TN 37831, USA

[c]National Center for Computational Toxicology, Office of Research and Development, U.S. Environmental Protection Agency, Research Triangle Park, NC, 27711, USA

Abstract

In support of the Endocrine Disruptor Screening Program (EDSP), the U.S.EPA's Office of Research and Development (ORD) is developing high-throughput screening (HTS) approaches to identify chemicals that alter target sites in the thyroid hormone (TH) pathway. The sodium iodide symporter (NIS) is a transmembrane glycoprotein that mediates iodide uptake into the thyroid as the initial step of TH biosynthesis. Previously, we screened 293 ToxCast chemicals (ph1v2) using a HEK293T cell line expressing human NIS in parallel radioactive iodide uptake (RAIU) and cell viability assays to identify potential environmental NIS inhibitors. Here, we expanded NIS inhibitor screening for a set of 768 ToxCast Phase II (ph2) chemicals, and applied a novel computational toxicology approach based on the ToxPrint chemotype to identify chemical substructures associated with NIS inhibition. Following single-concentration screening (at 1×10^{-4}M with a 20% inhibition cutoff), 235 samples (228 chemicals) were further tested in multiple-concentration (1×10^{-9} - 1×10^{-4}M) format in both RAIU and cell viability assays. The 167 chemicals that exhibited significant RAIU inhibition were then prioritized using combined RAIU and cell viability responses that were normalized relative to the known NIS inhibitor sodium perchlorate. Some of the highest ranked chemicals, such as PFOS, tributyltin chloride, and triclocarban, have been previously reported to be thyroid disruptors. In addition, several novel chemicals were identified as potent NIS inhibitors. The present results were combined with the

*Corresponding authors. laws.susan@epa.gov (S.C. Laws), stoker.tammy@epa.gov (T.E. Stoker).

Supplementary data to this article can be found online at https://doi.org/10.1016/j.envint.2019.02.024.

Conflict of interest statement
The authors declare no conflict of interest.

Disclaimer
The views expressed in this paper are those of the authors and do not necessarily reflect the views or policies of the U.S. Environmental Protection Agency.

previous ph1v2 screening results to produce two sets of binary hit-calls for 1028 unique chemicals, consisting of 273 positives exhibiting significant RAIU inhibition, and 63 positives following application of a cell viability filter. A ToxPrint chemotype-enrichment analysis identified > 20 distinct chemical substructural features, represented in > 60% of the active chemicals, as significantly enriched in each NIS inhibition hit-call space. A shared set of 9 chemotypes enriched in both hit-call sets indicates stable chemotype signals (insensitive to cytotoxicity filters) that can help guide structure-activity relationship (SAR) investigations and inform future research.

Keywords

Sodium-iodide symporter; Thyroid; Endocrine disruptor; High-throughput *in vitro* screening assay; ToxPrint; Chemotype

1. Introduction

Endocrine disrupting chemicals (EDCs) in the environment are associated with adverse health effects, especially when exposure occurs during critical periods of reproduction and development. Despite strong evidence that xenobiotics can perturb thyroid hormone (TH) signaling and TH-regulated physiological and developmental functions (Boas et al., 2012; Brucker-Davis, 1998; Capen and Martin, 1989; DeVito et al., 1999; Gilbert et al., 2016; Olker et al., 2018a), progress with investigating thyroid disruption has been slowed due to a lack of available *in vitro* methods to evaluate the array of thyroid molecular target sites. Unlike disruption of the estrogen and androgen hormone pathways, where structurally diverse groups of chemicals are known to interact primarily with ligand-nuclear receptor binding (Grimaldi et al., 2015), thyroid-disruptive chemicals do not typically target the thyroid hormone receptor. Instead, thyroid target sites primarily include TH synthesis, secretion, transport, and metabolism (Ferrari et al., 2017; Hornung et al., 2015; Maurício Martins da et al., 2018; Murk et al., 2013; Pearce et al., 2013). For this reason, there has been a recent global effort to develop and implement the use of high throughput screening (HTS) assays to expand the coverage of molecular targets of thyroid-disrupting chemicals (Dong and Wade, 2017; Murk et al., 2013; OECD, 2017). The current project is part of a joint effort between the U.S. EPA's Endocrine Disruptor Screening Program (EDSP) and Office of Research and Development (ORD) to expedite the use of HTS and computational toxicology to evaluate chemicals under the Agency's regulatory purview for thyroid-disrupting activity. To date, significant progress has been made by developing assays to screen three well-known targets of thyroid disruption, producing a significant quantity of *in vitro* data for identifying inhibitors of human sodium-iodide symporter (NIS), thyroid peroxidase and deiodinases (Hallinger et al., 2017; Hornung et al., 2018; Olker et al., 2018b; Paul Friedman et al., 2016; Paul et al., 2014; Wang et al., 2018).

The NIS mediates iodide uptake into the thyroid gland, the initial step for TH biosynthesis (Carrasco, 1993). Though high-resolution protein structure is unavailable, mutagenesis studies and homologous modeling suggest NIS to be a glycoprotein with 13 transmembrane helices (Dai et al., 1996; Darrouzet et al., 2014; Levy et al., 1998). NIS function in the thyroid is dependent upon Na^+/K^+ ATPase to maintain the cross-membrane electrochemical

gradient of Na^+ to cotransport two Na^+ cations with one I^- anion (Carrasco, 1993; Eskandari et al., 1997), and to concentrate [I^-] 20–40 fold greater than serum levels (Dohán et al., 2003). NIS is also expressed in the mammary gland, stomach, and salivary gland, though its function in these tissues remains to be elucidated (Darrouzet et al., 2014; Jhiang et al., 1998; Kotani et al., 1998; Tazebay et al., 2000).

Monovalent anions such as the environmental contaminants perchlorate (ClO_4^-), thiocyanate (SCN^-), and nitrate (NO_3^-) are known to competitively inhibit NIS function (De Groef et al., 2006). NIS can also transport other monovalent anions including ClO_3^-, $SeCN^-$, ReO_4^-, TcO_4^-, Br^-, and BF_4^- (Dohán et al., 2007; Eskandari et al., 1997). Exposure to several of these anions has been shown to disrupt TH synthesis in humans (Greer et al., 2002; Horton et al., 2015; Leung et al., 2010) and other vertebrates (Ortiz-Santaliestra and Sparling, 2007; Stoker et al., 2006). Until recently, knowledge of NIS inhibition activity among environmental chemicals was limited to inorganic anions, whereas the activity of most organic pollutants had not been investigated. As part of a major research effort to fill this data gap, we recently validated and applied a high-throughput radioactive iodide uptake (RAIU) *in vitro* assay (Hallinger et al., 2017) to the screening of 293 ToxCast chemicals, constituting the ph1v2 portion of the ToxCast Phase II library (note that most of the ph1v2 chemicals were previously screened in Phase I of the ToxCast program and, thus, have previously been referred to by us as Phase I chemicals). This first screening set predominately consisted of pesticides and herbicides (Richard et al., 2016; Wang et al., 2018).

In this study, we expanded the chemical space for NIS inhibitor screening to include 768 new ph2 inventory chemicals from the ToxCast Phase II library, and applied a novel computational toxicology approach based on the ToxPrint chemotype to identify chemical substructures associated with NIS inhibition. The ph2 chemical library incorporates a more diverse set of 768 environmental, industrial and pharmaceutical compounds, which unlike the previously screened ph1v2 library (293 compounds), had little to no previous toxicological information (Richard et al., 2016). Based on the RAIU assay results, chemicals were quantitatively ranked using a previously developed, toxicity-adjusted approach (Wang et al., 2018) that incorporates potencies of both RAIU inhibition and cytotoxicity. The present results were then combined with the previous ph1v2 results to produce two sets of binary hit-calls for a total of 1028 unique chemicals: positive hit-calls in the first set consisting of those chemicals exhibiting significant RAIU inhibition, whereas hit-calls in the second set comprised a reduced subset following application of a cell viability filter. These two sets of hit-call results (with and without a cell viability filter) were used for exploration of enrichments of NIS inhibitors in both chemical use-category space and substructure feature space. For the latter, we employed a publicly available set of chemical substructural features, termed ToxPrint chemotypes, that were specifically designed for profiling and analyzing environmentally relevant chemical inventories such as ToxCast (Yang et al., 2015) and can be used in safety assessment and data-mining applications (Al Sharif et al., 2017).

This study reports the results from the screening of 768 ToxCast ph2 chemicals for their ability to inhibit the NIS-mediated uptake of iodide and potentially alter thyroid hormone synthesis. This is also the first study in computational toxicology to identify specific

chemical substructures that could be associated with NIS inhibition. ToxPrint chemotype-enrichment analysis of the combined results for the ToxCast Phase II sub-inventories, ph1v2 and ph2, highlights specific chemical substructures that may be associated with NIS inhibition to potentially provide new understanding of the mechanistic underpinnings of the NIS biological target interaction.

2. Materials and methods

2.1. ToxCast chemical inventory definitions

Phase I of the ToxCast program screened a set of 310, mostly pesticidal active chemicals (ph1v1 inventory) across hundreds of assays. At the conclusion of Phase I, a slightly smaller version of this inventory, consisting of 293 chemicals, was reprocured and moved into broader Phase II testing; this chemical set, referred to as ph1v2, was the subject of our earlier NIS screening study (Wang et al., 2018). Phase II testing also included an expanded set of 768 chemicals (ph2) spanning a more diverse set of industrial and commercial chemicals. The present study reports the results of screening of this ph2 chemical set. Chemical inventories associated with each of the ToxCast testing phases (I, II, III) are described in (Richard et al., 2016), and associate chemical structure files are available for download at https://comptox.epa.gov/dashboard/chemical_lists/toxcast.

2.2. Chemical library preparation

Chemicals from the ToxCast Phase II library (ph 2 subset) were obtained from the National Center for Computational Toxicology (NCCT), U.S. EPA. The test library contained 777 samples, representing 768 unique chemicals; 9 chemicals were in duplicate to serve as internal quality controls. Chemicals were solubilized in dimethyl sulfoxide (DMSO) ($\leq 2 \times 10^{-2}$M, Table S1) and supplied in thirteen 96-well plates (62 samples per plate) (Evotec Inc., Branford, CT). Stock chemical plates were visually inspected under an inverted microscope to confirm solubility in each well (Table S1). All control chemicals, including sodium perchlorate ($NaClO_4$), sodium nitrate ($NaNO_3$), sodium thiocyanate (NaSCN), 2,4-dichlorophenoxyacetic acid (2,4-D), and 2,3-dichloro-1,4-napthoquinone (DCNQ) (Sigma Aldrich, St. Louis, MO), were initially solubilized in DMSO (EMD Millipore Corp., Darmstadt, Germany) at 2×10^{-2}M. All chemicals in the ToxCast inventory supplied for testing undergo manual quality curation review prior to registration in EPA's DSSTox structure database (Richard et al., 2016), and are assigned DSSTox chemical identifiers (DTXSIDs, chemical names, CAS numbers) and mapped to chemical structures (DTXCIDs), wherever possible. These identifiers and maximum concentrations used in this study are provided in Table S1.

2.3. Chemical screening

To maximize resources and testing efficiency, chemicals were screened by a tiered approach (Fig. 1) described previously (Wang et al., 2018). A total of 777 blinded samples were initially screened in single-concentration radioactive iodide uptake (RAIU) assay at 1×10^{-4}M with some exceptions owing to solubility (Table S1). A total of 235 samples that produced median RAIU inhibition > 20% were further tested in parallel RAIU and cell viability assays at six concentrations (1×10^{-9} - 1×10^{-4}M, obtained from

10-fold serial dilutions beginning with the maximum concentration, Table S1). Cell culture preparation and assays followed previously described protocols (Hallinger et al., 2017). Briefly, low passage hNIS-HEK293T-EPA cells (< 25 passes) were grown for 40 h in ScintiPlate-96 microplates (Perkin Elmer, Waltham, MA) and 96-well solid white assay plates (Corning, Corning, NY) for the RAIU and cell viability assays, respectively. A critical modification in the protocol to ensure cell adherence was to coat all 96-well plates with high molecular weight 0.01% poly-L-lysine (Sigma, St. Louis, MO) and wash with sterile deionized H_2O prior to cell seeding. After growth, cells were subjected to 2 h of chemical exposure at room temperature (in addition to 0.05 μCi/well radioactive ^{125}I in the RAIU assay), followed by ice-cold uptake buffer washing to terminate the exposure. RAIU was quantified by measuring intracellular ^{125}I counts per minute (CPM) with a MicroBeta^2 microplate scintillation counter (Perkin Elmer, Waltham, MA). Cell viability was measured via CellTiter-Glo (Promega, Fitchburg, WI) and BMG FLUOstar Omega, where luminescent signal was quantified as relative light units (RLU) indicative of ATP level.

To monitor the performance of RAIU and cell viability assays, multiple control chemicals were included in each assay plate; $NaNO_3$ (RAIU assay EC_{80} control), NaSCN (RAIU assay EC_{20} control), and 2,4-D (RAIU assay negative control) were included at 1×10^{-4}M, while $NaClO_4$ (RAIU assay positive control) and DCNQ (cell viability assay positive control) were included with six concentrations (1×10^{-9} - 1×10^{-4}M). All assays were conducted in three independent runs using separate passages of hNIS-HEK293T-EPA cells (i.e., 3 biological replicates). The assay plate maps for single and multi-concentration screening are provided in Fig. S1.

2.4. Screening data analysis

The full details of data analysis methods have been previously described (Wang et al., 2018). Chemical identities were blinded during the screening process. RAIU and cell viability assay raw values were normalized per 96-well plate as the percent activity of the median DMSO control values. In single-concentration screening, the median of normalized percent activity from the 3 biological replicates for each chemical was used to determine whether the chemical would be further evaluated in multiple-concentration testing. The median value was chosen over the mean value in the analysis for its resistance to the impact of extreme values or outliers. A 20% RAIU inhibition threshold was used to select chemicals for multi-concentration testing. This threshold was determined based on the variation of DMSO vehicle control, i.e., the 3 times the median absolute deviation (3bMAD, b = 1.4826) calculated using DMSO wells from all 39 single-concentration assay plates. As the 3bMAD of DMSO was calculated to be 17.91%, the value for the inhibition threshold was rounded to 20% to move chemicals forward for additional multiple-concentration testing.

In multiple-concentration screening, the activity thresholds (14.51% for cell viability, 23.57% for RAIU) were the 3bMAD calculated using the responses of the two lowest concentrations across all test chemicals (i.e. responses at 1×10^{-9} and 1×10^{-8}M). The calling of positives for RAIU inhibition and cytotoxic activity was solely based on multi-concentration test results. Dose-response curves were fit for active chemicals using the Hill model specified in U.S. EPA's ToxCast pipeline (Filer et al., 2017). Chemicals that produced

significant RAIU inhibition were also analyzed using a toxicity-adjusted potency ranking approach (Wang et al., 2018). In brief, chemicals were prioritized by ranking scores that were calculated by the numeric sum of two values: 1) the area between the dose-response curves of RAIU and cell viability; and 2) the distance between median responses of RAIU and cell viability at the highest concentration tested. Scores were normalized as percentage of that observed for the reference chemical, NaClO4, which has a ranking score set at 200.

Coefficients of variation (CV) of DMSO, Z' scores (Zhang et al., 1999) and AC_{50} of positive controls (calculated using $NaClO_4$ for RAIU, DCNQ for cell viability) were calculated for each assay plate to monitor assay performance. Test results would be rejected if one or more of the following criteria were met: 1) CV of DMSO of the corresponding plate was > 15%, 2) Z' < 0.5, 3) $\log AC_{50}$ of positive control deviated > 0.5 from the historical average value. For potency reporting, both AC_{50} (the log concentration where the modeled activity equals 50% of the modeled maximal activity) and absolute EC_{50} ($absEC_{50}$, log concentration where the modeled activity equals 50% of control activity) were included. For chemicals that demonstrated significant cytotoxicity, the concentration where cell viability dropped below the 3bMAD (14.51%) is reported as the cytotox-point (equivalent of $absEC_{85.49}$ for cell viability). All analysis was performed in R (ver 3.4.3) using the toxplot package (Wang, 2018; Wang et al., 2018).

2.5. ToxPrint Chemotype enrichment analysis

The enrichment analyses were performed using HTS results for chemicals from the current study combined with results from our previous screening of the ToxCast ph1v2 chemical set (Wang et al., 2018). A list of 1028 unique chemicals (Table S4) was generated by merging results for replicate test samples (as internal quality controls) and removing substances that could not be assigned a discrete structure (e.g., mixtures etc.). Based on the screening results, two sets of RAIU inhibition hit-calls were generated for the enrichment analyses: actives in the Hit1 set are defined as the 273 positive chemicals (27%) exhibiting significant RAIU inhibition in multiple-concentration assays; actives in the Hit2 set are a subset of the Hit1 actives following application of a cell viability filter, consisting of 63 chemicals (6%) that exhibited non-cytotoxic RAIU inhibition at one or more test concentrations. Significance of activity was determined using 3bMAD values as thresholds. For chemicals that were tested in replicated samples, the hit-calls were assigned as positive if at least one of the samples was positive.

To evaluate the possible impact of chemical substructural features influencing both positive and negative assay results, the ToxPrint chemotype enrichment analysis workflow (CTEW) was applied to the Hit1 and Hit2 sets of NIS inhibitor screening results. The CTEW approach is designed to identify enriched local chemical-activity signals within structurally (and potentially mechanistically) diverse bioassay datasets, such as those generated in association with the ToxCast program. The CTEW employed the publicly available ToxPrint chemotype (CT) set (https://chemotyper.org/) that was developed by Altamira (Altamira, Columbus, OH USA) and Molecular Networks (Molecular Networks, Erlangen, GmbH) under contract from the U.S. Food and Drug Administration. ToxPrints consist of 729 sub-structural features (i.e., chemotypes) to allow for representation of chemicals in binary

fingerprints (0 or 1, representing if a chemotype is absent or present). ToxPrints are designed to capture a broad diversity of chemical atom, bond, chain, and scaffold types, as well as to represent chemical patterns and properties especially relevant to various toxicity and safety assessment concerns (Yang et al., 2015).

For analyzing the NIS screening results, the two sets of RAIU inhibition hit-calls were presented in binary form (1 = positive, 0 = negative, Table S4) and submitted as two separated analyses to the CTEW implemented in Python. The CTEW first generated a binary CT fingerprint table for all 1028 chemicals, which was then used to generate a confusion matrix (i.e., a 2 × 2 table that reports counts of true positives, true negatives, false positives, and false negatives) for each CT in association with the corresponding set of binary RAIU inhibition hit-calls, where the following definitions apply: true positives (TP) were chemicals that contain the CT and had positive hit-calls; true negatives (TN) had neither the CT nor positive hit-calls; false positives (FP) contain the CT but had negative hit-calls; and false negatives (FN) do not contain the CT but had positive hit-calls. To determine if a CT was enriched, a set of statistics was calculated to filter out insignificant results while retaining both weak and strong enrichments for follow-up analysis. These applied filtering thresholds included: Odds Ratio (OR) ≥ 3, one-tailed Fisher's exact p-value ≤0.05, and number of True Positives ≤3, where: $OR = (TP \times TN)/(FN \times FP)$. In addition, a Balanced Accuracy (BA) was computed as $BA = 0.5 \times (TP/(TP + FN) + TN/(TN + FP))$ for each individual enriched CT, as well as for the ensemble of all enriched CTs above the applied thresholds; the latter representing a global model that indicates the ability of the full set of enriched CTs to predict RAIU inhibition activity. Lastly, inverse CTEW enrichment analyses were conducted in which the RAIU inhibition binary hit-calls [1,0] were reversed [0,1] to explore CTs enriched in the negative space of the assay results (i.e., statistically enriched in non-hits). An enriched CT in the negative hit space was termed as CT-INV.

2.6. Use-category enrichment analysis

For describing the primary use of chemicals, use-categories for ToxCast Phase II chemicals were retrieved from a previous study (Strickland et al., 2018) and are listed in Table S4. Use-categories were initially defined in the Chemical Products Categories (CPCat) database (Dionisio et al., 2015) and are publicly available on EPA's CompTox Dashboard (https://comptox.epa.gov/dashboard/). During the enrichment analysis, only the top 10 use-categories (by chemical representation) were kept, with the remaining re-categorized as “other”. A use-category was considered enriched if the in-category hit rate was significantly larger than the overall hit rates (i.e., the hit rate in the 1028 chemicals).

3. Results

3.1. Assay performance

To ensure the quality of the assay data, each 96-well assay plate was evaluated using reference/control chemical responses and additional calculated quality control (QC) metrics. Summaries of these plate-wise measures indicated the overall good performance in both single and multi-concentration screening assays. The responses of vehicle control DMSO, RAIU EC_{20} and EC_{80} control NaSCN and NaNO3, and negative control 2,4-D demonstrated

high stability and low variability across the assays (Fig. S2 and Table S2). In addition, the QC metrics including CV of DMSO, Z' scores, and AC_{50} of positive controls ($NaClO_4$ for RAIU, DCNQ for cell viability) also demonstrated the robustness of the assays (Table S3). The Z' score for RAIU assay averaged 0.78 and 0.80 in single- and multiple-concentration screening, respectively. Similarly, the AC_{50s} for positive controls demonstrated excellent reproducibility across the assays, with standard deviations of ≤0.13 (logM) for both RAIU and cell viability assays.

In addition to the plate-wise QC measures, the 9 internally replicated ToxCast chemicals allowed further estimation of intra-assay reproducibility (Fig. S3). All replicated samples demonstrated similar responses in single-concentration RAIU assays except for clorophene. The inactivity observed for the source sample of clorophene was confirmed as due to insufficient sample in the chemical mother plate for chemical transfer and testing (Table S1, Sample ID: TP001686C05). Overall, theses quality-control measures indicate the screening assays were reliably delivering low background variation, excellent dynamic range and reproducibility.

3.2. RAIU inhibition and potency ranking

A total of 777 blinded samples (768 unique chemicals) initially screened at 1×10^{-4}M in the RAIU assay produced inhibitory responses ranging from 2.3% to 122.3% of the DMSO vehicle control (Fig. 2). Most chemical samples (69.8%) produced < 20% RAIU inhibition, whereas only 15.1% (117) produced > 50% RAIU inhibition. Based on a 20% inhibition threshold, 235 samples (228 chemicals) were further tested in multiple-concentration RAIU and cell viability assays.

In multiple-concentration testing, cell viability assays were conducted in parallel with the RAIU assays to identify responses that may be confounded by cytotoxicity, and significant activity thresholds were determined by 3bMAD values of each assay (23.57% inhibition for RAIU assay and 14.51% inhibition for cell viability assay). Among the 235 samples tested in multiple-concentration, 172 (including replicates, 167 unique chemicals) demonstrated significant RAIU inhibition response. Based on the 3bMAD, only 12 of the 172 samples that actively inhibited RAIU did not cause significant cytotoxicity at any of the concentrations tested. Dose-response curves for all chemicals are provided in Fig. S4.

The dose-response of the 172 samples that produced significant RAIU inhibition were further analyzed using our previously developed ranking system, which reports a normalized (in reference to $NaClO_4$) potency ranking score that incorporates both RAIU and cytotoxic activities (Wang et al., 2018). All multiple-concentration testing and ranking results are shown in Table S1, and the top 15 chemical samples are shown in Table 1. The ranking scores, along with the dose-response of reference chemical $NaClO_4$ and the top 15 ranked chemical samples are shown in Fig. 3. Most of these chemicals produced much weaker RAIU inhibitions than $NaClO_4$. With the reference chemical $NaClO_4$ assigned a score of 200, the 172 test chemical samples received ranking scores from 179.7 to −57.6, with only 3 having ranking score > 100, 25 having ranking score between 50 and 100, and 145 having ranking score < 50. Among the 172 chemical samples, 26 (25 unique chemicals) produced non-cytotoxic RAIU inhibition at one or more concentrations. These 26 chemical samples

are shown in blue in Fig. 3a. Most of the 26 samples received high rankings, and 5 of them produced > 50% RAIU inhibition at concentrations not confounded by cytotoxicity. Since the background variation of the cell viability assays in this screening was very small (3bMAD = 14.51%), if the activity threshold was adjusted to 20%, a common threshold used for *in vitro* cell viability assays (ex. OECD Guideline H295R Steroidogenesis Assay (OECD, 2011)), then 54 of the 172 samples produced RAIU inhibition without cytotoxicity at one or more concentrations (Table S1) and 13 produced over 50% RAIU inhibition without cytotoxicity.

3.3. Enrichment of use-categories in ToxCast phase II NIS-inhibition actives

Combining the NIS-inhibition assay outcomes from the current and previous NIS inhibitor screening (Wang et al., 2018) yielded results for 1028 unique ToxCast Phase II chemicals. A total of 273 chemicals exhibited significant RAIU inhibition in multi-concentration tests (positives in the Hit1 set), which accounted for 27% of the entire test library. However, if cell viability is considered (using 3bMAD as threshold), then only 63 (6%) of chemicals demonstrated non-cytotoxic RAIU inhibition at one or more concentrations (positives in the Hit2 set).

A use-category for each test compound (Table S4) was assigned based on the Chemical Products Categories (CPCat) database (Dionisio et al., 2015) to represent primary use for each hit set chemical (Fig. 4). Although the ToxCast Phase II (ph1v2 & ph 2 subsets) library has a large number of pharmaceuticals and chemical intermediates (Fig. 4A), these two categories account for significantly less proportion in the Hit1 (Fig. 4B) and Hit2 (Fig. 4C) actives. The other three abundant categories herbicides, pesticides and microbicides, remain as dominant in the list of Hit1 and Hit2 actives. The categories food-flavor-fragrance and solvent only have two actives for each in Hit1, and are no longer present in the Hit2 actives. The percentage of actives within each use-category along with the overall hit rates are shown in Fig. 5. The use-categories pesticide and microbicide, were enriched in both the Hit1 and Hit2 active sets, relative to the total test sets. The degree of enrichment (i.e., the difference between in-category hit rate and overall hit rate) also drastically decreases for use-category pesticide, microbicide, surfactant from Hit1 to Hit2 sets, which is expected as chemicals in these subgroups have been shown to decrease cell viability in a number of *in vitro* assays.

3.4. Enrichment of ToxPrint chemotypes in ToxCast phase II NIS-inhibition actives

The two sets of binary NIS inhibition assay hit-calls for the 1028 total chemicals (Table S4) were submitted for CTEW analysis to: 1) identify both positive (CT) and negative (CT-INV) enrichments; 2) determine enriched CTs common to both sets, despite the 4-fold reduction in the percentage of positives in the Hit2 set; and 3) assess the effect of the cell viability filter on the overall enriched CT-positive balanced accuracy (i.e., BA for Hit1 vs. Hit2).

CTEW results for the NIS-inhibition Hit1 set yielded a total of 30 positively enriched ToxPrint CTs and 7 CT-INVs enriched in negatives. Complete lists of CTs, CT-INVs and enrichment statistics for the Hit1 set are provided in Tables S5 and S6. The ToxPrint fingerprint matrix listing chemicals in the test set along with indication of their enriched CTs is provided in Table S7. Among the more highly represented and significant CTs

were biphenyls (Txp-474, 479), aromatic amines (Txp-108, 109), aromatic and alkyl/alkenyl halides (Txp-141, 142, 144, 184), and metals and organotins (Txp-5, 6, 324, 338, 340). To provide an approximate indication of coverage, one or more of these 30 positively enriched CTs are present in 161 chemicals, or 59% of the positives in the Hit1 set, and 50 of the 61 chemicals (82%) containing 2 or more enriched CTs are correctly predicted positive in the Hit1 set. An overall Balanced Accuracy (BA) of 0.70, computed using the full set of 30 positively enriched CTs (i.e., chemical predicted positive if it contains 1 or more CTs), indicates reasonable global predictivity of the full set of CTs. Closer examination of the 30 enriched CTs also indicated that 10 CTs were sufficiently inter-related such that the overall BA was unaffected by their omission. For example, Txp-137, bond:CX_halide_alkenyl-Cl_dichloro_(1_1-) and Txp-140, bond:CX_halide_alkenyl-X_dihalo_(1_1-) are related ToxPrints (the former is nested in the latter), present in the same 6 chemicals within the NIS-inhibition test set, so one could be excluded. Finally, inclusion of the 7 enriched CT-INVs, 5 of which pertain to alcohols (Txp-118, 127, 128, 130, 131), had negligible impact on the overall BA.

CTEW results for the NIS Hit2 set, where positives were a subset of those in the Hit1 set, yielded a total of 23 enriched ToxPrint CTs and 9 enriched CT-INVs (Tables S8, S9 and S10). Although the overall rate of True Positives (TPs) for this much smaller active space was slightly higher than for the Hit1 set, at 78% (49/63 correctly predicted active), there were many more False Positives (FPs) predicted by the presence of 1 or more of the 23 enriched CTs (235). The overall BA of the full set of enriched CTs (78%) was slightly higher than the Hit1 set, indicating slightly better overall predictivity. Some CTs that were found to be enriched in the larger Hit1 set, such as biphenyls (Txp-474, 479), aromatic amines (Txp-108, 109), and pyrrolidones (Txp-614), were no longer found to be enriched in the cell-viability filtered Hit2 subset, whereas nitriles (Txp-15) and several CTs pertaining to trihaloalkyl-containing compounds (Txp-146, 152, 169, 171) were newly enriched in the smaller Hit2 subset. Recall that enrichment is determined relative to the overall hit rates, which for Hit1 and Hit2 sets are quite different – 27% and 6%, respectively; hence, a correspondingly larger percentage of CT-actives is required in the Hit1 space to qualify as enrichment.

4. Discussion

The use of blinded sample identities and plate-wise assay performance criteria in this study provided data of the highest quality and confidence, as shown by the high Z' scores and low variability in vehicle controls in both the single- and multi-concentration RAIU screenings. The internal chemical replicates also demonstrated consistent responses that further support strong assay reproducibility. Generation of these rigorous data is essential for the subsequent computational toxicology analyses including chemical potency ranking and chemotype enrichment analysis.

The highest ranked chemical, phenolphthalein, is commonly used as an indicator in acid-base titrations, but has also been used as a laxative drug. Although it has been withdrawn from the U.S. market due to carcinogenicity risks, it is still prescribed for constipation patients in areas such as China, as well as having been identified in weight-

loss supplements (Baofang et al., 2015; Coogan et al., 2000). To date, there is no report in the literature regarding the potential of phenolphthalein to interfere with the thyroid system. Our finding is the first to show that phenolphthalein can disrupt NIS-mediated iodide uptake. Phenolphthalein demonstrated borderline cytotoxicity yet very strong RAIU inhibition potency, with an AC_{50} of −6.14 (logM), which was only slightly weaker than the reference chemical $NaClO_4$ (AC_{50} of −6.31). Future studies are warranted to determine whether phenolphthalein can alter thyroid hormone synthesis and cause adverse effects *in vivo*.

Several perfluoroalkyl substances (PFAS), including PFOS, PFOS-K, and potassium perfluorohexanesulfonate (PFHS-K), received high ranking scores with either nominal or no cytotoxicity in the NIS inhibitor screening (Fig. 3b, Table 1), though their RAIU inhibition potencies were nearly two orders of magnitude weaker than the reference chemical, $NaClO_4$. Both PFOS-K and PFHS-K were tested for the first time for NIS inhibition potentials, whereas PFOS had been previously tested as part of the earlier ToxCast ph1v2 library screening (Wang et al., 2018). Although the two PFOS samples in this study showed slightly different responses, the higher ranked sample had a similar dose-response with the PFOS (free acid) previously tested. PFOS-K is the potassium salt form of PFOS and demonstrated nearly identical responses, suggesting that the acidity of PFOS does not impact the performance of the *in vitro* cell assays. PFHS-K has a shorter carbon chain (C6) compared to PFOS (C8), yet showed similar responses to PFOS with nearly identical AC_{50} values (−4.73 vs. −4.75, log M). This result is also the first to report that PFHS-K has the potential to interfere with NIS-mediated iodide uptake. The ToxCast Phase II library tested here also included several other PFAS (marked in green in Table S1) but most of them, including PFOA, were inactive or showed low activity in the screening. Although PFAS are ubiquitous and persistent in the environment and in human/animal tissues, and there is evidence of PFAS disrupting thyroid function (Lau, 2015), interpretation of the NIS inhibition results for these PFAS requires additional review and follow-up study. In particular, the mechanism of the observed RAIU inhibition by PFOS and PFHS-K needs further clarification to determine whether the NIS protein is directly targeted. PFOS and PFHS-K have surfactant properties and may affect the function of NIS as a membrane protein by increasing the fluidity of the cell membrane (Hu et al., 2003; Xie et al., 2010).

Other highly ranked toxicants evaluated in the NIS inhibitor screening included several herbicides and antimicrobials. One of these, dinoseb, is an herbicide banned in the EU and USA for teratogenicity and has been reported to reduce T4 serum levels in the rat (Cunha and van Ravenzwaay, 2005). However, in this study dinoseb demonstrated an atypical dose-response in the RAIU assay that may have been caused by a reduction in ATP rather than a direct NIS inhibition. Specifically, dinoseb is an oxidative phosphorylation uncoupler that interferes cellular ATP production, which could disrupt the cross-membrane Na^+ gradient that NIS depends on by interfering with the function of Na^+/K^+ ATPase (Salla et al., 2017). Tributyltin chloride is another top-ranked chemical that has been shown to cause hypo-thyroidal effects *in vivo* and to activate the thyroid receptor *in vitro* (Sharan et al., 2014). Triclocarban is an antibacterial agent that was previously shown to be a non-competitive NIS inhibitor in rat thyroid follicular cells (Wu et al., 2016) and had a high rank in this study. For the remaining top-ranked chemicals shown

in Fig. 3, including benz(a)anthracene, nitrofen, hexachlorocyclopentadiene, mepanipyrim, 4-chloro-1,2-diaminobenzene, nelivaptan, and zamifenacin, we were unable to find any reports of thyroid disruption activity in the literature. [Note: because the stock sample of benz(a)anthracene was observed to have precipitation, the potency result in this study could be underestimated.]

One of the main goals of generating such a large *in vitro* data set for thyroid endpoints is to be able to take advantage of computational toxicology approaches to explore possible structural-activity relationships. In this study, the present results for the ph 2 library were combined with the previous ph1v2 library screening results to produce two sets of binary hit-calls for 1028 unique ToxCast Phase II chemicals and analyzed using the ToxPrint chemotype-enrichment analysis. Despite observed differences in results for the Hit1 and Hit2 sets, we found 11 common CTs and 3 CT-INVs significantly enriched in both Hit1 and Hit2 sets. Figs. 6 and 8 graphically present the corresponding enrichment percentages (above baseline activity rate) for the top 9 common CTs (2 redundant CTs are not shown) and 3 CT-INVs in the Hit1 and Hit2 sets, along with the size of the CT-subsets (i.e., total number of chemicals containing the CT in the test set indicated by the small blue circle), which impacts the p-value statistically. Interestingly, the common Hit1 and Hit2 CT set contains an ortho-halogenated diphenyl ether CT (Txp-184, bond:CX_halide_aromatic-X_ether_aromatic_(Ph-O-Ph)_generic) whereas the biphenyl CT (Txp-479, chain:aromaticAlkane_Ph-C1-Ph) is only found enriched in the Hit1 set, without the cell viability filter applied. Images of two enriched CTs (Txp-142, 184) are displayed to the right of Fig. 6. Fig. 7 shows Txp-184 (and Txp-142) superimposed on the 12 chemicals containing this CT, along with their activity status in both the Hit1 and Hit2 datasets. Several of these chemicals, including oxyfluorfen, nitrofen, cyhalofop-butyl and triclosan were highly ranked in the NIS inhibitor screening. In addition, this CT was found to be positively enriched in 85 other ToxCast HTS assays and these results could provide a basis for exploring putative biological target associations with NIS-inhibition or effects on thyroid hormone synthesis. Finally, if we consider the common set of 3 alcohol-containing CT-INVs in Fig. 8, we note that the top CT (bond:CO-H_alcohol_aliphatic_generic) is a general aliphatic form that encompasses both the primary and secondary alkyl subset. A total of 129/144 (90%) of the chemicals containing this CT are inactive in the Hit1 set, whereas 143/144 (99%) are inactive in the Hit2 set.

These initial CTEW results indicate significant enrichment signal in both the Hit1 and Hit2 results sets and provide support to the objective of the Hit2 cell viability filtering step, which is to focus the assay outcome to a set of mechanistically clean positives, with potentially more clearly defined structure-activity domains. Even with a 75% reduction in the number of actives in the Hit2 set, there was only a reduction of 25% in the number of enriched CTs (from 30 to 23), with 11 CTs common in both sets, indicating significant remaining and stable structure-activity “signal”. CTs found enriched in the Hit1 set, but no longer enriched in the cell-viability filtered Hit2 set also point to chemical features that may be more sensitive to cell-viability influences, pointing to chemical activity domains that could be further probed.

In summary, the use of the NIS HTS approach can identify chemicals that have the potential to inhibit the NIS and the ranking system can be used to prioritize the chemicals for further evaluation in both orthogonal assays and short-term *in vivo* studies. Here, we report the NIS inhibitor screening for 768 ToxCast ph2 chemicals. The 172 chemicals that were active in the RAIU assay were ranked based on potency, effects on cell viability, and normalized to perchlorate. Only 25 chemicals had non-cytotoxic RAIU inhibition at one or more concentrations. Some of the highest ranked chemicals included PFOS, tributyltin chloride, and triclocarban, which have been shown to disrupt the thyroid axis. We also report the first computational toxicology study that identifies specific chemical substructures associated with NIS inhibition. The present results in combination with the previous ph1v2 library screening results produced two sets of binary hit-calls for 1028 unique chemicals, consisting of 273 positives exhibiting significant RAIU inhibition, and 63 positives following application of a cell viability filter. A ToxPrint chemotype-enrichment analysis identified > 20 distinct chemical substructure features associated with each version of the NIS inhibition hit-call space. A shared set of 9 unique ToxPrint chemotypes enriched in both hit-call sets indicates strong chemotype signals that are insensitive to cell viability filters, that can help guide SAR investigations and inform future experiments. This chemotype information and SAR for both active and inactive chemicals will be used to test predictions in the NIS screening of the E1K ToxCast library of over 800 chemicals and guide follow-up studies.

Supplementary Material

Refer to Web version on PubMed Central for supplementary material.

Acknowledgements

This research was funded by the Office of Research and Development, U.S. EPA, Washington, DC. The authors thank U.S. EPA scientists Dr. Steve Simmons for assistance with developing the hNIS-HEK293T-EPA cell line, Dr. Michael Hornung and Dr. Timothy Shafer for their scientific and editorial contributions to this manuscript.

Abbreviations:

EDSP	Endocrine Disruptor Screening Program
ToxCast	Toxicity Forecaster
CV	coefficient of variation
NIS	sodium iodide symporter
RAIU	radioactive iodide uptake
RLU	relative light unit
SD	standard deviation
T_3	triiodothyronine
T_4	thyroxine

TH	thyroid hormone
3bMAD	three times the baseline median absolute deviation
DMSO	dimethylsulfoxide
2,4-D	2,4-dichlorophenoxyacetic acid
DCNQ	2,3-dichloro-1,4-napthoquinone
HEK	human embryonic kidney
AOP	adverse outcome pathway
HTS	high-throughput screening
PFOS	perfluorooctanesulfonic acid
PFOA	perfluorooctanoic acid
CT	chemotype

References

Al Sharif M, Tsakovska I, Pajeva I, Alov P, Fioravanzo E, Bassan A, Kovarich S, Yang C, Mostrag-Szlichtyng A, Vitcheva V, Worth AP, Richarz A-N, Cronin MTD, 2017. The application of molecular modelling in the safety assessment of chemicals: a case study on ligand-dependent PPARγ dysregulation. Toxicology 392, 140–154. 10.1016/j.tox.2016.01.009. [PubMed: 26836498]

Baofang L, Jianmin Z, Jianwei S, 2015. What makes the phenolphthalein still be a safe drug for patients in China? Pharmacoepidemiol. Drug Saf 24, 555–557. 10.1002/pds.3777. [PubMed: 25906829]

Boas M, Feldt-Rasmussen U, Main KM, 2012. Thyroid effects of endocrine disrupting chemicals. Mol. Cell. Endocrinol 355, 240–248. 10.1016/j.mce.2011.09.005. [PubMed: 21939731]

Brucker-Davis F, 1998. Effects of environmental synthetic chemicals on thyroid function. Thyroid 8, 827–856. 10.1089/thy.1998.8.827. [PubMed: 9777756]

Capen CC, Martin SL, 1989. The effects of xenobiotics on the structure and function of thyroid follicular and C-cells. Toxicol. Pathol 17, 266–293. 10.1177/019262338901700205. [PubMed: 2675279]

Carrasco N, 1993. Iodide transport in the thyroid gland. Biochim. Biophys. Acta Rev. Biomembr 1154, 65–82. 10.1016/0304-4157(93)90017-I.

Coogan PF, Rosenberg L, Palmer JR, Strom BL, Zauber AG, Stolley PD, Shapiro S, 2000. Phenolphthalein laxatives and risk of cancer. J. Natl. Cancer Inst 92, 1943–1944. 10.1093/jnci/92.23.1943. [PubMed: 11106687]

Cunha GC-P, van Ravenzwaay B, 2005. Evaluation of mechanisms inducing thyroid toxicity and the ability of the enhanced OECD test guideline 407 to detect these changes. Arch. Toxicol 79, 390–405. 10.1007/s00204-004-0644-2. [PubMed: 15692820]

Dai G, Levy O, Carrasco N, 1996. Cloning and characterization of the thyroid iodide transporter. Nature 379, 458–460. 10.1038/379458a0. [PubMed: 8559252]

Darrouzet E, Lindenthal S, Marcellin D, Pellequer JL, Pourcher T, 2014. The sodium/iodide symporter: state of the art of its molecular characterization. Biochim. Biophys. Acta 1838, 244–253. 10.1016/j.bbamem.2013.08.013. [PubMed: 23988430]

De Groef B, Decallonne BR, Van der Geyten S, Darras VM, Bouillon R, 2006. Perchlorate versus other environmental sodium/iodide symporter inhibitors: potential thyroid-related health effects. Eur. J. Endocrinol 155, 17–25. 10.1530/eje.1.02190. [PubMed: 16793945]

DeVito M, Biegel L, Brouwer A, Brown S, Brucker-Davis F, Cheek AO, Christensen R, Colborn T, Cooke P, Crissman J, Crofton K, Doerge D, Gray E, Hauser P, Hurley P, Kohn M, Lazar J, McMaster S, McClain M, McConnell E, Meier C, Miller R, Tietge J, Tyl R, 1999. Screening methods for thyroid hormone disruptors. Environ. Health Perspect 107, 407–415. 10.2307/3434545. [PubMed: 10210697]

Dionisio KL, Frame AM, Goldsmith M-R, Wambaugh JF, Liddell A, Cathey T, Smith D, Vail J, Ernstoff AS, Fantke P, Jolliet O, Judson RS, 2015. Exploring consumer exposure pathways and patterns of use for chemicals in the environment. Toxicol. Rep 2, 228–237. 10.1016/j.toxrep.2014.12.009. [PubMed: 28962356]

Dohán O, De la Vieja A, Paroder V, Riedel C, Artani M, Reed M, Ginter CS, Carrasco N, 2003. The sodium/iodide symporter (NIS): characterization, regulation, and medical significance. Endocr. Rev 24, 48–77. 10.1210/er.2001-0029. [PubMed: 12588808]

Dohán O, Portulano C, Basquin C, Reyna-Neyra A, Amzel LM, Carrasco N, 2007. The Na+/I− symporter (NIS) mediates electroneutral active transport of the environmental pollutant perchlorate. Proc. Natl. Acad. Sci 104, 20250–20255. 10.1073/pnas.0707207104. [PubMed: 18077370]

Dong H, Wade MG, 2017. Application of a nonradioactive assay for high throughput screening for inhibition of thyroid hormone uptake via the transmembrane transporter MCT8. Toxicol. in Vitro 40, 234–242. 10.1016/j.tiv.2017.01.014. [PubMed: 28119167]

Eskandari S, Loo DDF, Dai G, Levy O, Wright EM, Carrasco N, 1997. Thyroid Na+/I− symporter: mechanism, stoichiometry, and specificity. J. Biol. Chem 272, 27230–27238. 10.1074/jbc.272.43.27230. [PubMed: 9341168]

Ferrari SM, Fallahi P, Antonelli A, Benvenga S, 2017. Environmental issues in thyroid diseases. Front. Endocrinol 8. 10.3389/fendo.2017.00050.

Filer DL, Kothiya P, Setzer RW, Judson RS, Martin MT, 2017. tcpl: the ToxCast pipeline for high-throughput screening data. Bioinformatics 33, 618–620. 10.1093/bioinformatics/btw680. [PubMed: 27797781]

Gilbert ME, Sanchez-Huerta K, Wood C, 2016. Mild thyroid hormone insufficiency during development compromises activity-dependent neuroplasticity in the hippocampus of adult male rats. Endocrinology 157, 774–787. 10.1210/en.2015-1643. [PubMed: 26606422]

Greer MA, Goodman G, Pleus RC, Greer SE, 2002. Health effects assessment for environmental perchlorate contamination: the dose response for inhibition of thyroidal radioiodine uptake in humans. Environ. Health Perspect 110, 927. [PubMed: 12204829]

Grimaldi M, Boulahtouf A, Delfosse V, Thouennon E, Bourguet W, Balaguer P, 2015. Reporter cell lines for the characterization of the interactions between human nuclear receptors and endocrine disruptors. Front. Endocrinol 6. 10.3389/fendo.2015.00062.

Hallinger DR, Murr AS, Buckalew AR, Simmons SO, Stoker TE, Laws SC, 2017. Development of a screening approach to detect thyroid disrupting chemicals that inhibit the human sodium iodide symporter (NIS). Toxicol. in Vitro 40, 66–78. 10.1016/j.tiv.2016.12.006. [PubMed: 27979590]

Hornung MW, Kosian PA, Haselman JT, Korte JJ, Challis K, Macherla C, Nevalainen E, Degitz SJ, 2015. In vitro, ex vivo, and in vivo determination of thyroid hormone modulating activity of benzothiazoles. Toxicol. Sci 146, 254–264. 10.1093/toxsci/kfv090. [PubMed: 25953703]

Hornung MW, Korte JJ, Olker JH, Denny JS, Knutsen C, Hartig PC, Cardon MC, Degitz SJ, 2018. Screening the ToxCast phase 1 chemical library for inhibition of deiodinase type 1 activity. Toxicol. Sci 162, 570–581. 10.1093/toxsci/kfx279. [PubMed: 29228274]

Horton MK, Blount BC, Valentin-Blasini L, Wapner R, Whyatt R, Gennings C, Factor-Litvak P, 2015. CO-occurring exposure to perchlorate, nitrate and thiocyanate alters thyroid function in healthy pregnant women. Environ. Res 143, 1–9. 10.1016/j.envres.2015.09.013.

Hu W.y., Jones PD, DeCoen W, King L, Fraker P, Newsted J, Giesy JP, 2003. Alterations in cell membrane properties caused by perfluorinated compounds. Comp. Biochem. Physiol., Part C: Toxicol. Pharmacol 135, 77–88. 10.1016/S1532-0456(03)00043-7.

Jhiang SM, Cho J-Y, Ryu K-Y, DeYoung BR, Smanik PA, McGaughy VR, Fischer AH, Mazzaferri EL, 1998. An immunohistochemical study of Na+/I− symporter in human thyroid tissues and salivary gland tissues. Endocrinology 139, 4416–4419. 10.1210/endo.139.10.6329. [PubMed: 9751526]

Kotani T, Ogata Y, Yamamoto I, Aratake Y, Kawano J-I, Suganuma T, Ohtaki S, 1998. Characterization of gastric Na+/I− symporter of the rat. Clin. Immunol. Immunopathol 89, 271–278. 10.1006/clin.1998.4595. [PubMed: 9837697]

Lau C, 2015. Perfluorinated compounds: an overview. In: DeWitt JC (Ed.), Toxicological Effects of Perfluoroalkyl and Polyfluoroalkyl Substances. Springer International Publishing, Cham. 10.1007/978-3-319-15518-0_1.

Leung AM, Pearce EN, Braverman LE, 2010. Perchlorate, iodine and the thyroid. Best Pract. Res. Clin. Endocrinol. Metab 24, 133–141. [PubMed: 20172477]

Levy O, De la Vieja A, Ginter CS, Riedel C, Dai G, Carrasco N, 1998. N-linked glycosylation of the thyroid Na+/I− symporter (NIS). Implications for its secondary structure model. J. Biol. Chem 273, 22657–22663. 10.1074/jbc.273.35.22657. [PubMed: 9712895]

Maurício Martins da S, Lueni Lopes Felix X, Carlos Frederico Lima G, Ana Paula S-S, Francisca Diana P-M, Mariana Lopes de F, Rodrigo Soares F, Leandro M-A, Andrea Claudia Freitas F, 2018. Bisphenol A increases hydrogen peroxide generation by thyrocytes both in vivo and in vitro. Endocr. Connect 7, 1196–1207. 10.1530/EC-18-0348.

Murk AJ, Rijntjes E, Blaauboer BJ, Clewell R, Crofton KM, Dingemans MML, David Furlow J, Kavlock R, Köhrle J, Opitz R, Traas T, Visser TJ, Xia M, Gutleb AC, 2013. Mechanism-based testing strategy using in vitro approaches for identification of thyroid hormone disrupting chemicals. Toxicol. in Vitro 27, 1320–1346. 10.1016/j.tiv.2013.02.012. [PubMed: 23453986]

OECD, 2011. Test No. 456: H295R Steroidogenesis Assayin. 10.1787/9789264122642-en.

OECD, 2017. New Scoping Document on In Vitro and Ex Vivo Assays For the Identification of Modulators of Thyroid Hormone Signallingin. 10.1787/9789264274716-en.

Olker JH, Haselman JT, Kosian PA, Donnay KG, Korte JJ, Blanksma C, Hornung MW, Degitz SJ, 2018a. Evaluating iodide recycling inhibition as a novel molecular initiating event for thyroid axis disruption in amphibians. Toxicol. Sci 166, 318–331. 10.1093/toxsci/kfy203. [PubMed: 30137636]

Olker JH, Korte JJ, Denny JS, Hartig PC, Cardon MC, Knutsen CN, Kent PM, Christensen JP, Degitz SJ, Hornung MW, 2018b. Screening the ToxCast phase 1, phase 2, and e1k chemical libraries for inhibitors of iodothyronine deiodinases. Toxicol. Sci 10.1093/toxsci/kfy302.kfy302-kfy302.

Ortiz-Santaliestra ME, Sparling DW, 2007. Alteration of larval development and metamorphosis by nitrate and perchlorate in southern leopard frogs (Rana sphenocephala). Arch. Environ. Contam. Toxicol 53, 639–646. 10.1007/s00244-006-0277-y. [PubMed: 17657452]

Paul Friedman K, Watt ED, Hornung MW, Hedge JM, Judson RS, Crofton KM, Houck KA, Simmons SO, 2016. Tiered high-throughput screening approach to identify thyroperoxidase inhibitors within the ToxCast phase I and II chemical libraries. Toxicol. Sci 151, 160–180. 10.1093/toxsci/kfw034. [PubMed: 26884060]

Paul KB, Hedge JM, Rotroff DM, Hornung MW, Crofton KM, Simmons SO, 2014. Development of a thyroperoxidase inhibition assay for high-throughput screening. Chem. Res. Toxicol 27, 387–399. 10.1021/tx400310w. [PubMed: 24383450]

Pearce EN, Andersson M, Zimmermann MB, 2013. Global iodine nutrition: where do we stand in 2013? Thyroid 23, 523–528. 10.1089/thy.2013.0128. [PubMed: 23472655]

Richard AM, Judson RS, Houck KA, Grulke CM, Volarath P, Thillainadarajah I, Yang C, Rathman J, Martin MT, Wambaugh JF, Knudsen TB, Kancherla J, Mansouri K, Patlewicz G, Williams AJ, Little SB, Crofton KM, Thomas RS, 2016. ToxCast chemical landscape: paving the road to 21st century toxicology. Chem. Res. Toxicol 29, 1225–1251. 10.1021/acs.chemrestox.6b00135. [PubMed: 27367298]

Salla GBF, Bracht L, de Sá-Nakanishi AB, Parizotto AV, Bracht F, Peralta RM, Bracht A, 2017. Distribution, lipid-bilayer affinity and kinetics of the metabolic effects of dinoseb in the liver. Toxicol. Appl. Pharmacol 329, 259–271. 10.1016/j.taap.2017.06.013. [PubMed: 28624444]

Sharan S, Nikhil K, Roy P, 2014. Disruption of thyroid hormone functions by low dose exposure of tributyltin: an in vitro and in vivo approach. Gen. Comp. Endocrinol 206, 155–165. 10.1016/j.ygcen.2014.07.027. [PubMed: 25101840]

Stoker TE, Ferrell JM, Laws SC, Cooper RL, Buckalew A, 2006. Evaluation of ammonium perchlorate in the endocrine disruptor screening and testing program's male pubertal protocol: ability to

detect effects on thyroid endpoints. Toxicology 228, 58–65. 10.1016/j.tox.2006.08.026. [PubMed: 17011691]

Strickland JD, Martin MT, Richard AM, Houck KA, Shafer TJ, 2018. Screening the ToxCast phase II libraries for alterations in network function using cortical neurons grown on multi-well microelectrode array (mwMEA) plates. Arch. Toxicol 92, 487–500. 10.1007/s00204-017-2035-5. [PubMed: 28766123]

Tazebay UH, Wapnir IL, Levy O, Dohan O, Zuckier LS, Hua Zhao Q, Fu Deng H, Amenta PS, Fineberg S, Pestell RG, Carrasco N, 2000. The mammary gland iodide transporter is expressed during lactation and in breast cancer. Nat. Med 6, 871–878. [PubMed: 10932223]

Wang J, , 2018. ToxPlot R Package. Zenodo: Zenodo 10.5281/zenodo.1244736.

Wang J, Hallinger DR, Murr AS, Buckalew AR, Simmons SO, Laws SC, Stoker TE, 2018. High-throughput screening and quantitative chemical ranking for sodium-iodide symporter inhibitors in ToxCast phase I chemical library. Environ. Sci. Technol 52, 5417–5426. 10.1021/acs.est.7b06145. [PubMed: 29611697]

Wu Y, Beland FA, Fang J-L, 2016. Effect of triclosan, triclocarban, 2,2′,4,4′-tetrabromodiphenyl ether, and bisphenol A on the iodide uptake, thyroid peroxidase activity, and expression of genes involved in thyroid hormone synthesis. Toxicol. in Vitro 32, 310–319. 10.1016/j.tiv.2016.01.014. [PubMed: 26827900]

Xie W, Ludewig G, Wang K, Lehmler H-J, 2010. Model and cell membrane partitioning of perfluorooctanesulfonate is independent of the lipid chain length. Colloids Surf. B: Biointerfaces 76, 128–136. 10.1016/j.colsurfb.2009.10.025. [PubMed: 19932010]

Yang C, Tarkhov A, Marusczyk J, Bienfait B, Gasteiger J, Kleinoeder T, Magdziarz T, Sacher O, Schwab CH, Schwoebel J, Terfloth L, Arvidson K, Richard A, Worth A, Rathman J, 2015. New publicly available chemical query language, CSRML, to support chemotype representations for application to data mining and modeling. J. Chem. Inf. Model 55, 510–528. 10.1021/ci500667v. [PubMed: 25647539]

Zhang J-H, Chung TDY, Oldenburg KR, 1999. A simple statistical parameter for use in evaluation and validation of high throughput screening assays. J. Biomol. Screen 4, 67–73. 10.1177/108705719900400206. [PubMed: 10838414]

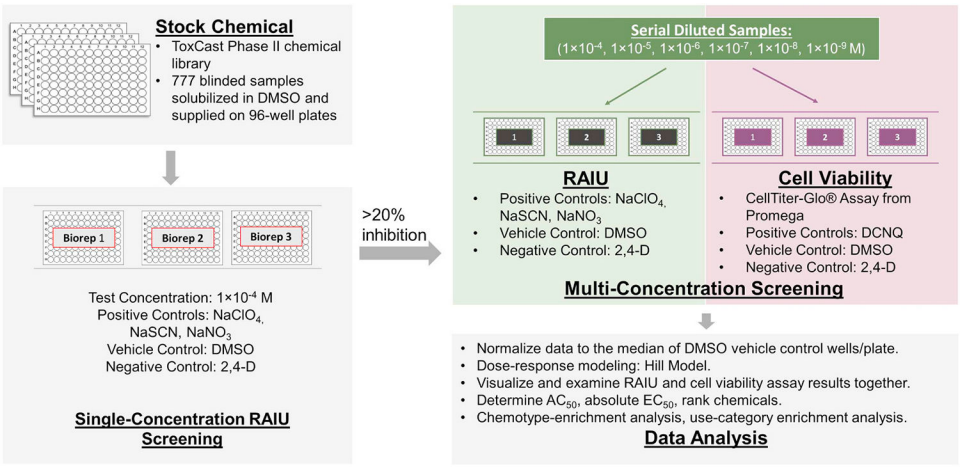

Fig. 1.

Workflow of the tiered high-throughput screening for identifying putative sodium-iodide symporter (NIS) inhibitors.

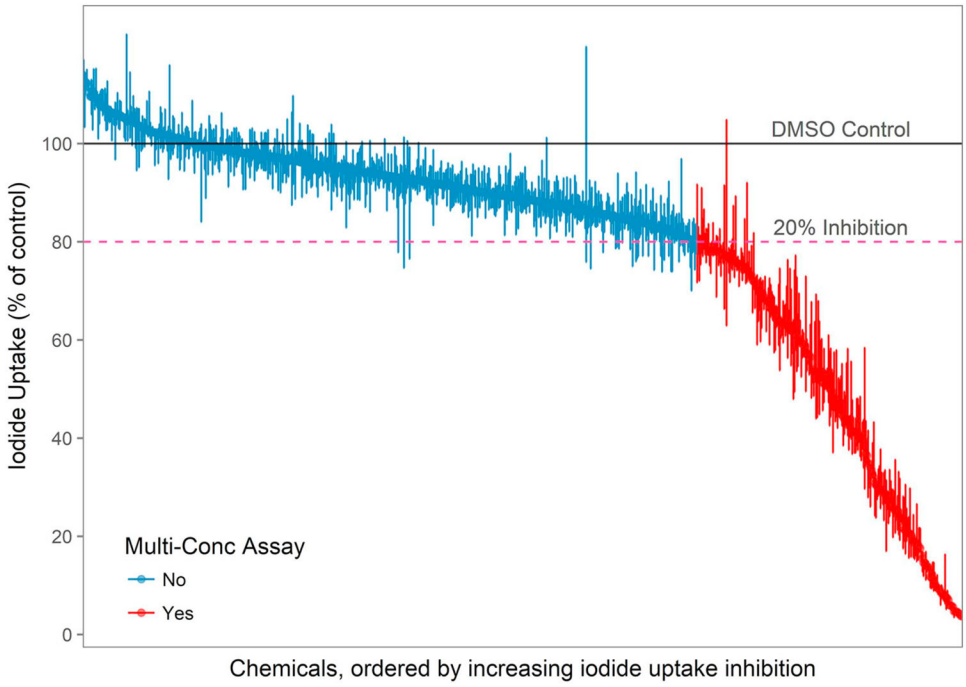

Fig. 2.

Median and range of test chemical responses in single-concentration RAIU screening. Median response of each chemical is represented by the dot and vertical bar shows the maximal and minimum iodide uptake. A pink horizontal line represents the 20% inhibition threshold. Of the 777 blinded chemical samples tested, 235 chemicals (30.2%) were selected for multiple-concentration testing based on 20% inhibition activity threshold.

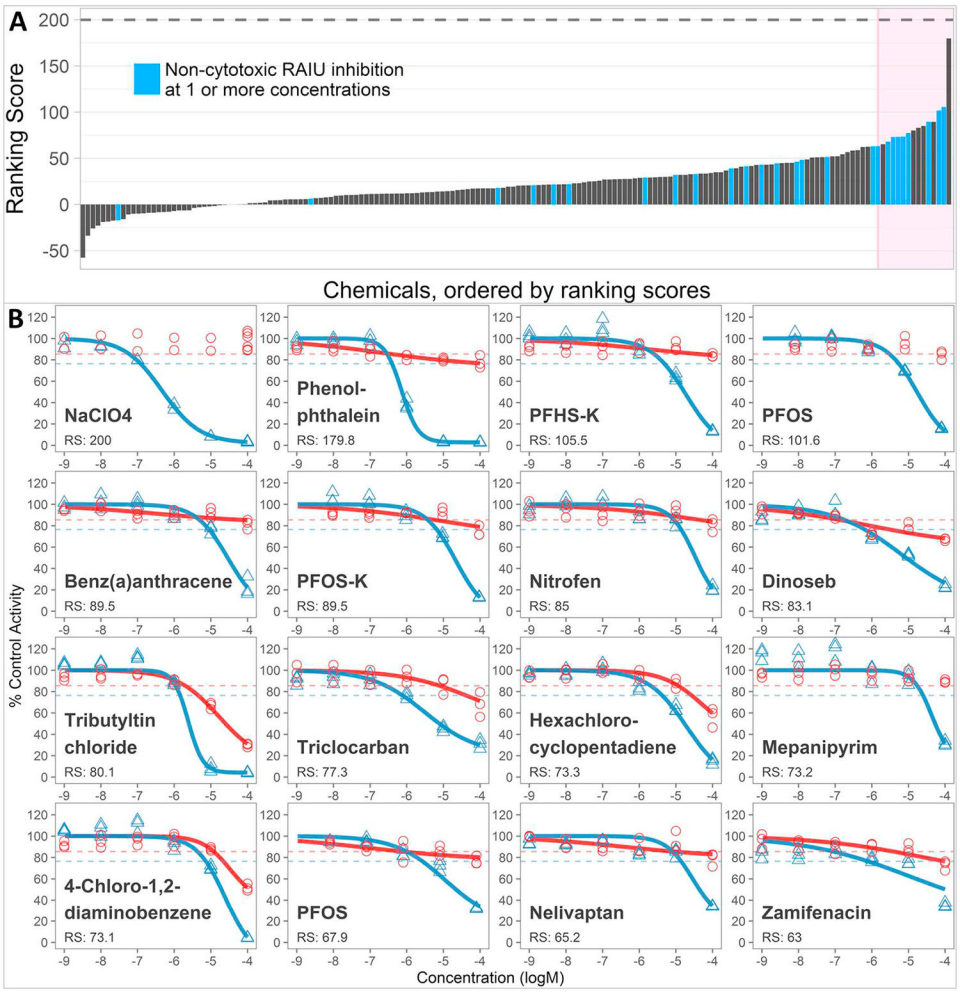

Fig. 3.

(A). Ranking scores for the 172 chemical samples that produced significant RAIU inhibition in multi-concentration screening. The 26 chemical samples that produced significant RAIU inhibition without any significant cytotoxicity (threshold 14.51% inhibition) at one or more concentrations are shown in blue. The top ranked 15 chemical samples are marked in pink rectangle. (B). Dose-response of reference chemical, $NaClO_4$ and top ranked 15 chemical samples. Dose-response curves were fitted only when significant inhibition occurred. Circle and red represent cell viability; triangle and blue represent RAIU. RS: ranking score.

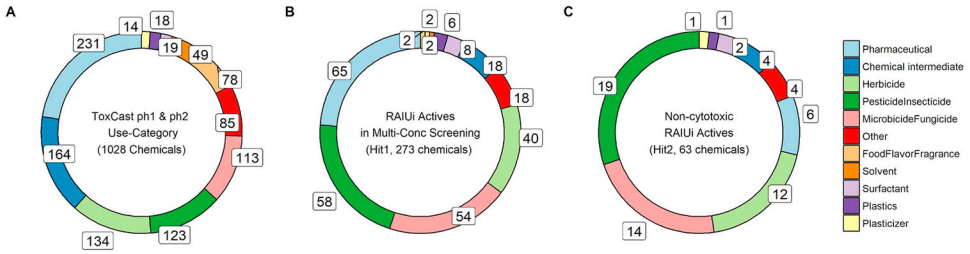

Fig. 4.

Distribution of use-categories for ToxCast Phase II (ph1v2, ph 2) chemicals. Only the top 10 use-categories (by chemical representation) are shown, with the remaining listed as “Other”; the numbers of chemicals in each use-category is labeled. (A) ToxCast ph1v2 and ph 2 full test set. (B) RAIU inhibition (RAIUi) active compounds in multi-concentration screening (Hit1 actives). (C) Non-cytotoxic RAIU inhibition active compounds in multi-concentration screening (Hit2 actives).

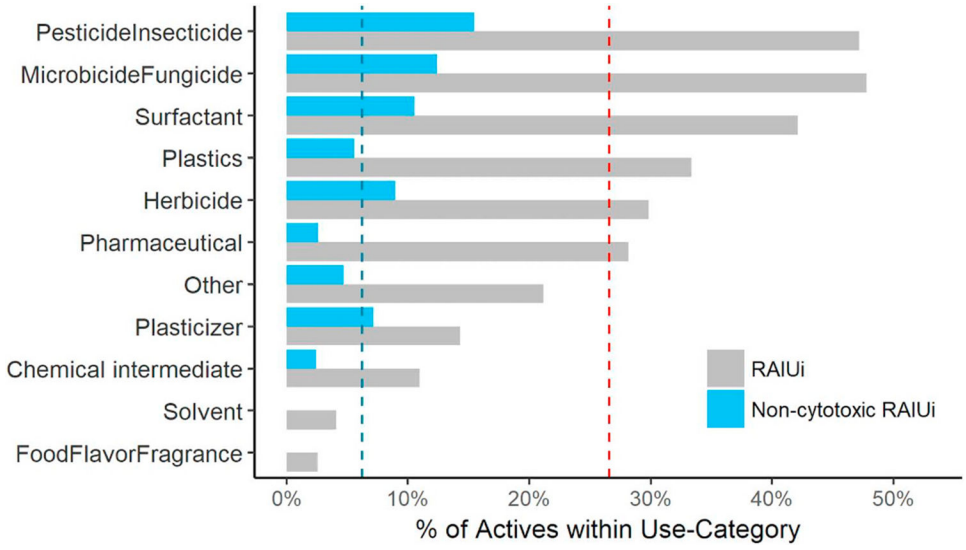

Fig. 5.

Percent of RAIU inhibition (RAIUi) actives within each use-category. A use-category was considered enriched if the in-category hit rate was significantly greater than the overall hit rates (i.e., the hit rate in the 1028 chemicals, 27% for RAIUi (Hit1), 6% for non-cytotoxic RAIUi (Hit2), represented by red and blue dotted vertical lines, respectively).

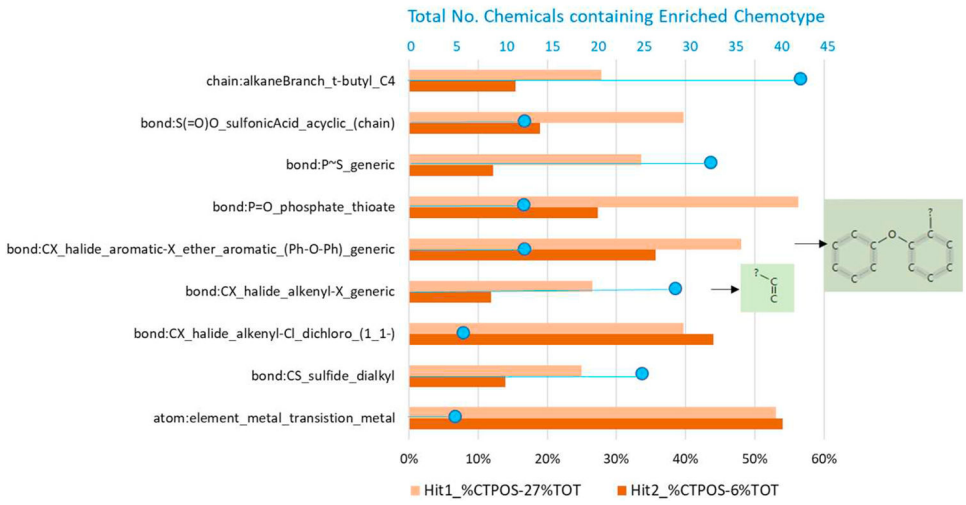

Fig. 6.

Common set of ToxPrint chemotype (CT) enrichments for NIS-inhibition Hit1 (light orange) and Hit2 (dark orange) assay activity sets showing enrichment of above baseline activity in each case, and the total number of chemicals containing the CT (blue line and circles). The baseline activity for Hit1 and Hit2 sets were 27% and 6%, respectively.

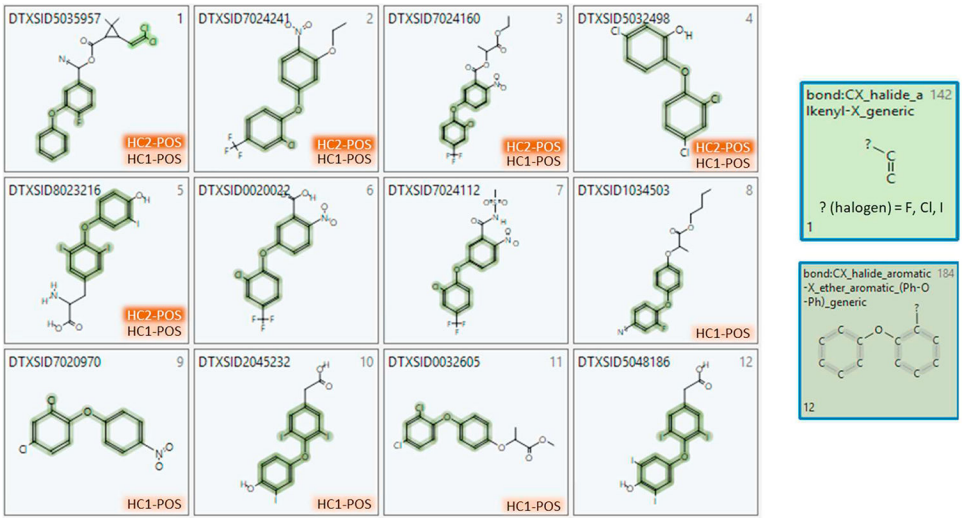

Fig. 7.

Chemicals in the NIS-Inhibition Phase II test set containing ToxPrint bond:CX_halide_aromatic-X_ether_aromatic_(Ph-O-Ph)_generic (Txp-184), with their activity status (POS) designated for Hit1 (HC1) and Hit2 (HC2) results (co-occurrence of Txp-142 is shown in one instance). Chemical names are: 1) cyfluthrin; 2) oxyfluorfen; 3) lactofen; 4) triclosan; 5) 3,5,3′-Triiodothyronine; 6) acifluorfen; 7) fomesafen; 8) cyhalofop-butyl; 9) nitrofen; 10) triatricol; 11) methyl (*RS*)-2-[4-(2,4-dichlorophenoxy)phenoxy]propionate; 12) tetrac.

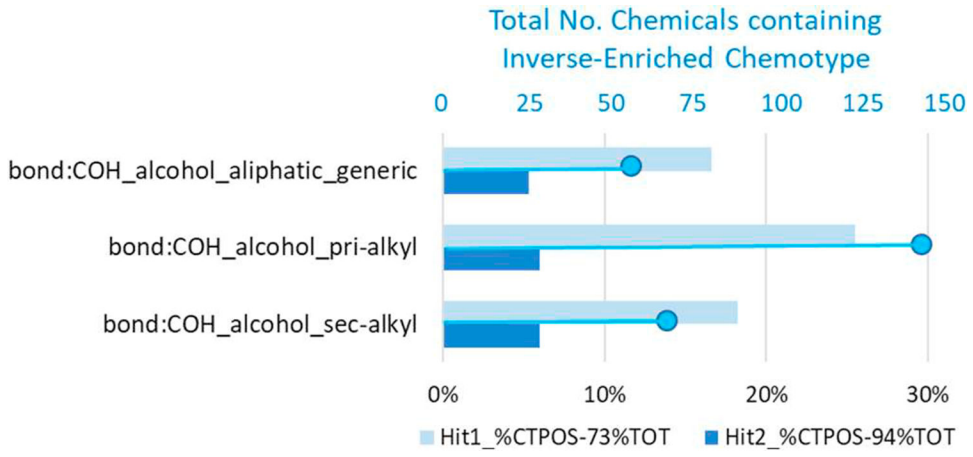

Fig. 8.

Common set of ToxPrint inverse-chemotype (CT-INV) enrichments for NIS-inhibition Hit1 (light blue) and Hit2 (dark blue) assay activity sets showing enrichment of above baseline activity in each case, and the total number of chemicals containing the CT (blue line and circles). The baseline activity for Hit1 and Hit2 sets were 73% and 94%, respectively.

Environ Int. Author manuscript; available in PMC 2022 May 09.

Table 1

Results for the top 15 ranked chemical samples that demonstrated significant RAIU inhibition in multi-concentration screening (as shown in Fig. 3B).

	Chemical	CAS NO.	Max Conc(M)[a]	AC50 (logM)	absEC50 (logM)	Cytotox-point[b]	Ranking score[d]	Non-cytotoxic RAIU inhibition at 1 or more conc[c]
1	Phenolphthalein	77-09-8	1×10^{-4}	−6.14	−6.13	−6.43	179.75	No
2	PFHS-K	3871-99-6	1×10^{-4}	−4.73	−4.77	−4.40	105.48	Yes
3	PFOS	1763-23-1	8×10^{-5}	−4.75	−4.77	NA	101.60	Yes
4	Benz(a)anthracene	56-55-3	1×10^{-4}	−4.53	−4.54	−4.16	89.49	No
5	PFOS-K	2795-39-3	9.5×10^{-5}	−4.67	−4.70	−5.24	89.48	Yes
6	Nitrofen	1836-75-5	1×10^{-4}	−4.48	−4.46	−4.35	85.03	No
7	Dinoseb	88-85-7	1×10^{-4}	−5.18	−5.06	−6.88	83.06	No
8	Tributyltin chloride	1461-22-9	1×10^{-4}	−5.61	−5.60	−5.70	80.06	No
9	Triclocarban	101-20-2	1×10^{-4}	−5.51	−5.11	−5.11	77.28	Yes
10	Hexachlorocyclo-pentadiene	77-47-4	1×10^{4}	−4.71	−4.77	−4.94	73.34	Yes
11	Mepanipyrim	110235-47-7	1×10^{-4}	−4.36	−4.27	NA	73.22	Yes
12	4-Chloro-1,2-diaminobenzene	95-83-0	1×10^{-4}	−4.61	−4.71	−4.92	73.09	Yes
13	PFOS	1763-23-1	8×10^{-5}	−4.95	−4.66	−6.11	67.90	Yes
14	Nelivaptan	439687-69-1	1×10^{-4}	−4.55	−4.36	−5.05	65.17	No
15	Zamifenacin	127308-82-1	1×10^{-4}	−4.97	NA	−5.40	63.02	Yes

Results for all test chemicals are in Table S1.

[a] Max Conc: the maximum permissible concentration tested in single-concentration screening. The Max Conc was obtained by 200 × dilution of the supplied stock chemicals (concentrations ≤2×10^{-2}M). Serial dilution of samples for multi-concentration assay started with the Max Conc. NA: not available, as no absEC$_{50}$ for RAIU was observed.

[b] Cytotox-point: the log concentration where significant reduction in cell viability (e.g, cytotoxicity, absEC$_{85.49}$) was observed. NA: not available, as no significant cytotoxicity was observed.

[c] Non-cytotoxic RAIU inhibition at 1 or more concentrations: Indicates chemicals that have significant RAIU inhibition without significant cytotoxicity at one or more concentrations tested in multi-concentration screening.

[d] Ranking score normalized to NaClO$_4$ (maximum ranking score of 200).